Journal of Visualization, Vol. 6, No.1 (2003) 9-20

Numerical Simulation of the Inner Structure of a Two-phase Plume Formed in a Stratification Environment

Chen, B. [*1], Song, Y. [*1] , Nishio, M.[*2] and Someya, S.[*2]

*1 Research Institute of Innovative Technology for the Earth, 9-2 Kizugawadai, Soraku-gun, Kyoto 619-0292, Japan.
e-mail: b.chen@aist.go.jp
*2 National Institute of Advanced Industrial Science and Technology, 1-2 Namiki, Tsukuba-shi, Ibaraki 305-8564, Japan.

Received 12 June 2002
Revised 9 September 2002

Abstract : The inner structure of a two-phase plume, driven by air bubble buoyancy and formed in a stratification ambient fluid in a rectangular tank, is numerically simulated by means of two-phase flow theory and Large-eddy simulation technology. Focusing on the discrete nature of the buoyant dispersed phase and on the role of momentum exchange between two phases during plume formation, we investigated the phenomena of mass "entraining-in" and "peeling-out" that occurs inside the stratified ambient plume. These phenomena are thought to result from an intricate interplay among phase interaction, static stability of the stratification ambient fluid itself, and dynamic stability due to turbulence. Numerical simulations show that there exists an inner-out structure of the stratified ambient plume, while at the same time predicting that the re-entraining-in mass flux is on the same order of magnitude as that of the inner peeling-out mass flux within the annular region centered around the plume. This further explains the mechanism underlying the formation of multi-scale eddies at the edge of the air bubble plume, which also constitutes the boundary between the inner and outer zones of this inner-out stratified fluid plume. Within the inner part of the plume, the mass entraining-in and peeling-out appeared as a spatial discontinuity. The numerically visualized three-dimensional density fields are consistent with the two-phase plume characteristics.

Keywords : Two-phase plume, Numerical simulation, LES, Stratification, Mass flux.

1. Introduction

Two-phase plumes are common buoyancy flow phenomena involved in hydraulic engineering and some environmental applications. Air bubble plumes applied to reservoir destratification (Schladow, 1993), CO_2 droplet plumes used in CO_2 ocean sequestration (Liro *et al.*, 1992; Haungan *et al.*, 1995), which is an option having enormous potential capacity to store anthropogenic CO_2, and deep-sea blowouts of oil and natural gas (Johansen, 1999) are some of the classical examples. Experimental results (Asaeda and Imberger, 1993; Socolofsky, 2000) have shown that the overall characteristics of

two-phase plumes are different from those of single-phase plumes, for which a self-similarity can be assumed, because the interactions between discrete bubbles or droplets and the continuous ambient fluid produce a multi-layer peeling structure. This is due to the slip velocities between bubbles/droplets and the ambient fluid, and the stability of the ambient stratification fluid itself. Based on the results of empirical investigations, theoretical models (McDougall, 1978; Asaeda and Imberger, 1993) were developed to describe the mean flow characteristics of continuous-phase plumes. These models were established by a set of ordinary differential equations with respect to a space coordinated vertically at the center of the plume. It also assumed that the plume is in steady flow and that the details of turbulence can be ignored. Some experimental constants, (e.g. entrainment coefficients and some parameters in the equation of mean velocity distribution along the plume section), were determined empirically. These models predicted some overall characteristics of a continuous plume, such as plume height, peeling height, and plume efficiency as a function of bubble/droplet releasing rate. However, there are almost no investigations in the literature of the inner physics of plume formation and ambient mass entraining-in and peeling-out, especially by means of numerical simulation. In this paper, we report our preliminary efforts to simulate and visualize two-phase plume formation and the inner behavior of ambient mass entraining and peeling by applying two-phase flow theories and large-eddy simulation technology.

This paper is organized as follows. First, the fundamental principles, governing equations, and numerical schemes applied in the model are introduced, and then the numerical results are validated using existing experimental data (Asaeda and Imberger, 1993) of mean density vertical profiles and the multi-layer outline structures of a continuous plume for different evolution times. Next, some typical three-dimensional fields are “visualized” in detail for density, ambient mass entraining-in flux and peeling-out flux, and streamlines. Finally, the formation mechanism and the inner interactions of the two-phase plume are discussed.

2. Theories, Governing Equations, and Numerical Schemes

Assuming that bubbles or droplets (dispersion phase) with mean diameter d_0 are released at height H from the bottom of a rectangular tank filled with stratification ambient fluid, the dynamics of the fluid elements for both continuous-phase fluid and discontinuous-phase fluid (bubbles or droplets) can be described, in principle, by theories of two-phase flows. Two alternate approaches are available for treating discontinuous-phase fluid (Sirignano, 1986). These are the Eulerian-Eulerian formulations (EEF) and Eulerian-Lagrangian formulations (ELF). The behavior of the discontinuous phase can be described originally by a so-called bubble/droplet number density function $f(t, X, d, u_{dj},\ldots)$, which is a function of time plus variables of spatial position vector, X, droplet diameter, d, droplet velocity vector, $\vec{u}_{dj}$, and other inter translation properties at the interface. The EEF is interpreted by integrating the partial differential equation $f(t, X, d, u_i,\ldots)$ according to the definition of averaging over a number of bubbles within the resolution scale, δx, larger than the space between bubbles, l. Strictly speaking, this averaging definition means that a discontinuous fluid is assumed to be as likely as a continuous fluid, and at the least, to be a pseudo-continuous fluid. The condition for this assumption, without losing the physical realization, is $l << \delta x << \boldsymbol{L}$, where $\boldsymbol{L}$ is the macro-spatial scale of the system. Then a group of partial differential equations consisting of bubble number density, volume fraction, and momentum for a pseudo-continuous fluid can be derived as a function of time and spatial coordinates. The resulting equations contain some corresponding source terms describing the statistical characteristics of discontinuous fluid within the resolution scale.

The other approach, ELF, takes into consideration the distribution of this number density function, $f(t, X, d, u_i,\ldots)$, approaching a delta function in the phase space. The characteristic ELF

equations are obtained in a straightforwardway, and these are a set of ordinary differential equations for discontinuous fluid itself. This is a popular scheme in two-fluid or two-phase flow studies for phenomena with a relatively short bubble/droplet injection time. With respect to the numerical scheme and current computer facilities, the memory size required by the ELF frame depends on the number of bubble/droplet groups, referred to as parcels, and on the amount of discontinuous fluid that might be implanted into the continuous fluid. For a two-phase flow with continuous air bubble injection, which is the case treated in the present study, the memory required for tracing continually injected air bubbles exceeds the memory capacity available at the current computer facility. Therefore, the EEF two-fluid approach was used in this study since it offers a more efficient representation. It is obvious, however, that the drawback of using the EEF approach is that it increases the difficulty and complexity of the numerical solution because two sets of partial differential equations, coupled with each other, must be solved numerically for the two phases.

The original force driving the dispersion motion is buoyancy, while the force acting on the stratified ambient fluid is drag force. The momentum interaction between dispersion and the stratified ambient fluid is governed by the respective momentum equations for each. Due to the relatively short time needed for air bubbles to rise from the tank bottom to the water free surface, and given the much lower solubility of air in water, mass change can be neglected in this study. Furthermore, thermal effects can also be neglected if the air bubbles are assumed to be at the same temperature as the water and dissolution heating is assumed not to occur (no mass change). This results in a condition where the bubble diameter remains constant, and for the sake of simplicity, bubble diameter can also be assumed to be equal to the diameter when initially injected if the effect of hydraulic pressure is also ignored. Finally, an additional mass conservative equation and a salinity mass fraction equation for the stratified ambient fluid as well as a void fraction equation for the quasi-continuous fluid, namely for the air bubbles, should be applied to the simulation to close the system mathematically.

Concerning the turbulence simulation generated in the central regime of the plume, we used large-eddy simulation technology to directly predict the instantaneous velocities and scalars on a spatial scale larger than the grid size while the sub-grid-scale motion and fluctuations of scalars are presented approximately by a structure-function model (Lesieur and Métais, 1996) for stratified fluid. For air bubbles, these terms are modeled by Smagorinsky's model.

Based on above physical model and the two-fluid theories, the governing equations of eddy-resolved variables, (^), normalized according to the scales of velocity (Uc), space (L) and time ($T=L/Uc$) for each phase, can be expressed by applying Schumann's filtering technique, in the *Eulerian-Eulerian* scheme, as follows. For the continuous phase, we have the general equations for conservation of mass and momentum, as:

$$\frac{\partial \overline{\rho}}{\partial t} + \frac{\partial \overline{\rho}\hat{\boldsymbol{u}}_i}{\partial \boldsymbol{x}_i} = \boldsymbol{0} \tag{1}$$

$$\frac{\partial \overline{\rho}\hat{u}_i}{\partial t} + \frac{\partial \overline{\rho}\hat{u}_i\hat{u}_j}{\partial x_j} = -\frac{\partial \hat{p}}{\partial x_i} + \frac{\partial \overline{\rho}\hat{\tau}_{ij}}{\partial x_j} + (\overline{\rho} - \rho_0)g_i + \left(\hat{F}_d\right)_i \tag{2}$$

where, p is defined by pressure (p_t) and hydrostatic pressure (p_h) as $p = p_t - p_h$ and satisfies the hydrostatic equation: $\partial p_h / \partial z = -\rho_o g$ where g_i is the acceleration due to gravity. $\hat{F}_d$ is the momentum exchange rate between the two phases, and will be defined later. For salinity, S, it is:

$$\frac{\partial \overline{\rho}\hat{\boldsymbol{S}}}{\partial \boldsymbol{t}} + \frac{\partial \overline{\rho}\hat{\boldsymbol{S}}\hat{\boldsymbol{u}}_j}{\partial \boldsymbol{x}_j} = \frac{\partial}{\partial \boldsymbol{x}_j}\left(\overline{\rho}\boldsymbol{D}_s \frac{\partial \hat{\boldsymbol{S}}}{\partial \boldsymbol{x}_j}\right) + \frac{\partial \overline{\rho}\hat{\boldsymbol{q}}_{Sj}}{\partial \boldsymbol{x}_j} \tag{3}$$

where D_s is the molecular diffusivity of salinity in water.

The governing equations derived for discontinuous fluid in the EEF satisfy the LES concept of

cut-off fitting:

$$\frac{\partial \hat{\alpha}}{\partial t} + \frac{\partial \hat{\alpha}\hat{u}_{dj}}{\partial x_j} = 0 \tag{4}$$

$$\frac{\partial \overline{\rho}_d \hat{u}_{di}}{\partial t} + \frac{\partial \overline{\rho}_d \hat{u}_{di}\hat{u}_{dj}}{\partial x_j} = \hat{\alpha}\left(\overline{\rho} - \rho_d\right)g_i + \left(\hat{F}_d\right)_i \tag{5}$$

where $\hat{\alpha}$ and $\hat{u}_{di}$ are the volume fraction and velocity vectors of discontinuous fluid, respectively. $\overline{\rho}_d = \hat{\alpha}\rho_d$, and ρ_d is the physical density of the discontinuous fluid.

To close this set of equations, the turbulent transport terms of the *Reynolds* stress tensor $\hat{\tau}_{ij}$ and *Reynolds* scalar flux $\hat{q}_s$ in sub-grid-scale; and momentum-exchange rate $\hat{F}_d$ have to be modeled in terms of resolved variables. The turbulent transport terms for stratified ambient fluid are expressed by the "structure-function" model (Lesieur and Métais, 1996) in order to take the effect of stratification into account:

$$\hat{\tau}_{ij} = \nu_{ti}\left(\frac{\partial \hat{u}_i}{\partial x_j} + \frac{\partial \hat{u}_j}{\partial x_i}\right) \tag{6}$$

$$\hat{q}_{sj} = \Gamma_{tj}\frac{\partial \hat{S}}{\partial x_j} \tag{7}$$

while the eddy viscosity, ν_{ti}, and the second order structure-function, F_{2i}, are expressed as:

$$\nu_{ti} = 0.105 C_K^{-3/2}\Delta x_i\left[F_{2i}\left(x, \Delta x\right)\right]^{1/2} \tag{8}$$

$$F_{2i}\left(x,\Delta x\right) = \langle \| \hat{u}_i(x,t) - \hat{u}_i(x+\Delta x,t) \|^2 \rangle \tag{9}$$

C_k =1.4. i = 1,2,3 corresponding to the horizontal (x and y directions, Fig.1) and vertical directions, respectively.

For air bubbles, Smagorinsky's model was employed to estimate turbulent SGS eddy viscosity, ν_{td}, which is given by:

$$\nu_{td} = \left(C_s\Delta\right)^2 / \hat{S}_{dij} / \hat{S}_{dij} \tag{10}$$

where Cs=0.05, which is reduced by about 25% from the normal value when dealing with bubble discontinuity, and $\hat{S}_{dij}$ is the strain rate of resolved eddies in the quasi-continuous fluid. The eddy diffusivities are modeled by:

$$\Gamma_{tj} = \frac{\nu_{tj}}{Pr_t} \tag{11}$$

where Pr_t is the turbulent *Prandtl* number.

The momentum-exchange rate is estimated by:

$$\hat{F}_d = 0.75\left(\pi/6\right)^{1/3}\rho_d \nu_w \hat{\alpha}^{2/3}\hat{n}_{d0}^{1/3} Cd \,/\, \hat{u}_j - \hat{u}_{dj} / \left(\hat{u}_j - \hat{u}_{dj}\right) \tag{12}$$

where ν_w is the kinematic viscosity of water, and the drag coefficient Cd is calculated by:

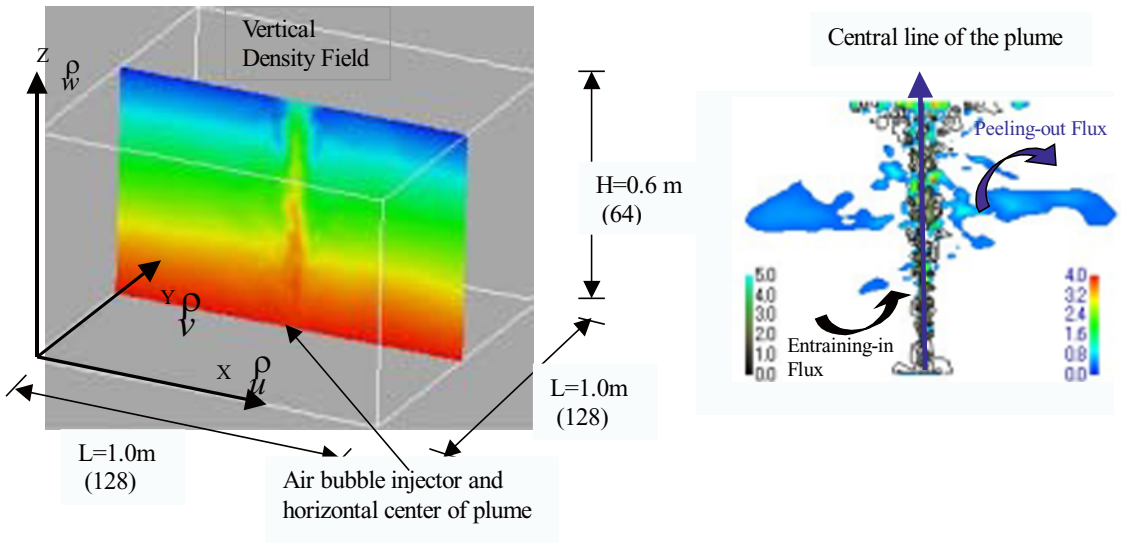

Fig. 1. Schematic representation of physical model and space coordinator system simulated in this study (left) and definition of entraining-in and peeling-out mass flux.

$$Cd = 24/Re_d \left(1. + 0.173\, Re_d^{0.657}\right) \tag{13}$$

where the *Reynolds* number Re_d is defined by the slip velocity and the diameter of the bubble.

The complete set of governing equations (6) ~ (13), together with equations (1)~(3) and (4)~(5) associated with the sub-models, is solved numerically using the so-called "Semi-implicit Method for Pressure-Linked Equations Consistent" (SIMPLEC) (Van Doormaal and Raithby, 1984). The algorithm is based on a finite control volume discretizating on a staggered grid system to ensure the preservation of the conservation properties of the original differential equations. A second-order central difference scheme was used for solving the momentum equations and a hybrid scheme of fourth-order central difference plus a "power-law" was used for the scalar equations in order to avoid grossly false values and to reduce numerical diffusion. The solution can be advanced in time by using an implicit second-order Adams-Bashforth scheme.

3. Model Validation

The physical model developed in this work and its associated programming were validated by simulating the results of a laboratory experiment on two-phase plumes formed in a stratified environment (Asaeda and Imberger, 1993). Figure 1 shows the physical model and spatial coordinate system used in the present study. The simulation domain is set to be 1.0 m×1.0 m×0.6 m in the horizontal and vertical directions, respectively, for a rectangular tank. A non-uniform grid of Nx=102, Ny=102, and Nz=64 points is used. The minimum grid size is 0.5×0.5×1.0 cm within the center of the domain (0.44 m×0.44 m×0.6 m) in which the bubble-releasing nozzle is located. The air bubbles are released into artificial seawater at a height of 4.0cm from the bottom at a release rate of 0.645×10^{-6} m^3/sec and an initial diameter of 1.05 mm. The initial ambient fluid stratification is created by applying a presumed salinity distribution in the vertical direction to a standard state equation of seawater (Unesco, 1981) to fit the experimental data. The initial buoyancy frequency is N^2=0.170 ($1/s^2$). The buoyancy frequency is defined as $N^2 = [-(g/\rho)(\partial\rho/\partial z)]^{1/2}$. The density is calculated in the simulation by solving the seawater state equation using updated salinity to handle the hydrostatic stability of the stratification ambient fluid. The boundary conditions at the water top surface (the free surface) are treated as a rigid slip wall according to Lam and Banerjee (1992), which is a

reasonable and simple way if no surface mass exchange occurs.

The mean density vertical profiles calculated by the model, at time T=312.0 seconds and T= 892.0 seconds after air bubble injection, are compared with experimental data in Fig.2 (left T=312.0 sec and right T=892.0 sec). It is apparent from the figure that the numerical predictions are in good agreement with the experimental data, although there exist some slight variances at heights around 0.5 m.

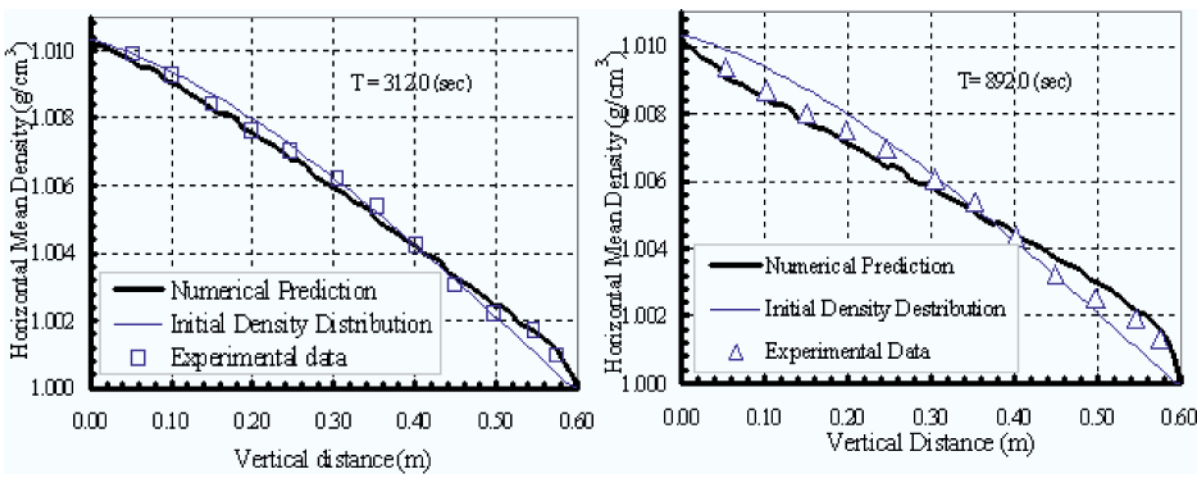

Fig. 2. Comparison of numerical simulation results of vertical density profiles averaged horizontally with experimental data (Asaeda and Imberger, 1993) at 312.0 seconds (left) and 890.0 seconds (right) after start of air bubble injection.

These variances may be related to some of the assumptions made in the simulation, namely that air bubble diameter remains constant, as well as to uncertainties about the water free surface boundary conditions. The basic overall characters of plume formation and evolution, for instance the intrusion position, are reasonably predicted when compared to the overall characteristics of the actual experimental results. The mechanism of mean density variation is that drag force, due to the raising air bubbles, which lift up the dense fluid from its hydraulic steady-position to a certain height so that the stratified ambient becomes destratified. In the early stage, the stratified fluid in the upper part of the tank was more quickly and effectively mixed vertically with the surrounding fluid because of the large scale top-surface flow, compared to fluid in the lower part of the tank. However, at time 892.0 seconds after the start of air bubble injection, the mean density in the lower part of the tank was significantly changed (Fig. 1 right) due to the large-scale motion created by the fluid impinging on the solid walls and being turned back from the walls. The details of plume development and the inner structure are discussed below.

4. Numerical Simulation of Inner Structure of Continuous-Phase Plume

After validation of the model and its programming, the numerical model was applied to investigate the inner structure and mechanism of plume development. In order to visualize the dynamic process whereby the dense fluid was driven upward by drag from the rising air bubbles before evolving into its own hydrostatic stability, we assumed that the plume was centered vertically with respect to the location of the air bubble injector, and the mass flux can then be defined as follows:

$$\vec{m}_f = \rho(\vec{u}+\vec{v}+\vec{w}) \tag{14}$$

The direction of the velocity vectors in equation(14) is defined in Fig. 1. Based on equation (14), we further define the entraining-in mass flux, m_{fin}, as one in which the horizontal velocity vectors, $\vec{U} = \vec{u} + \vec{v}$, are toward to the plume centerline while the peeling-out mass flux, m_{fout}, expressed by the horizontal velocity vectors, $\vec{U} = \vec{u} + \vec{v}$, is outward with respect to the plume centerline (Fig. 1, right). Using these definitions, the numerical simulation results of velocity and density were reexamined to produce the mass flux field.

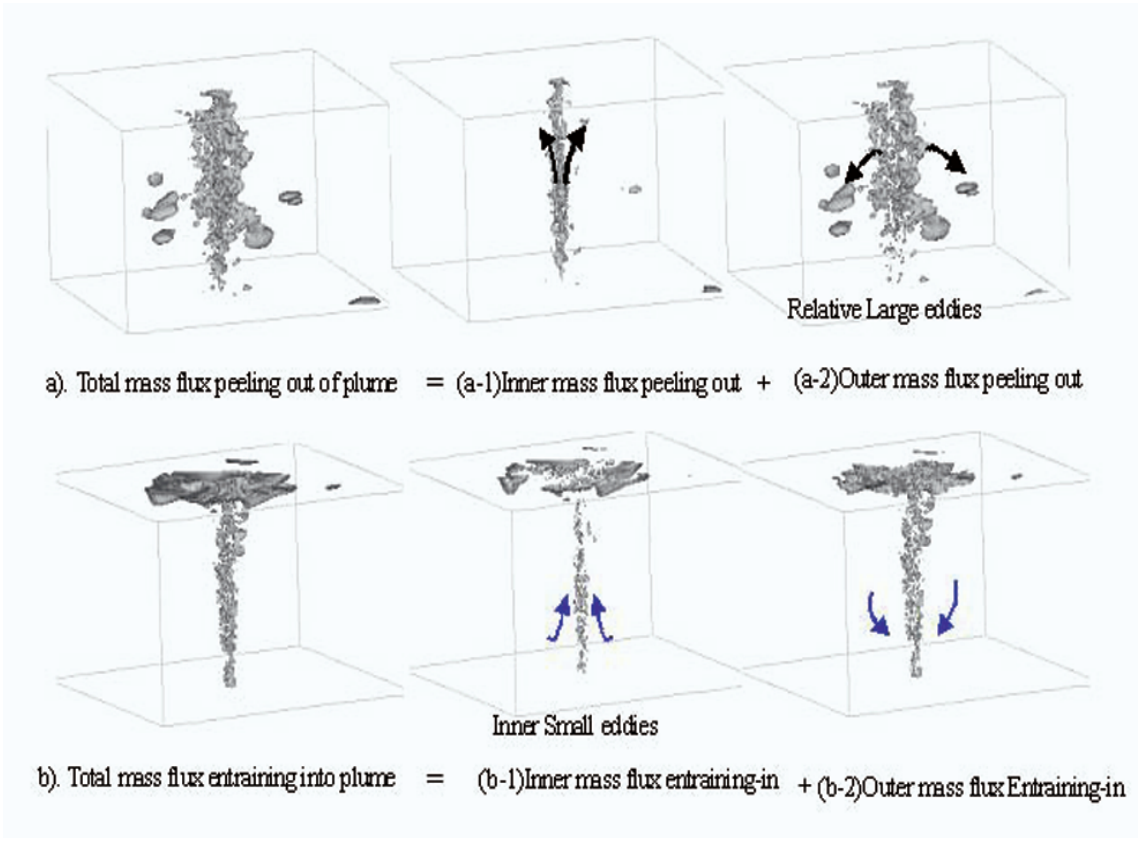

Fig. 3. 3-D visualization of peeling-out (top) and entraining-in (below) mass flux by iso-mass flux at 0.12 g/(cm^{2}sec).

To illustrate the spatial structure of the fully developed stratification fluid plume, the peeling-out mass flux (Fig.3a) and entraining-in mass flux (Fig.3b) at 521.0 sec after starting air bubble injection are visualized in three-dimensions by an iso-mass-flux with a value of 0.12 g/(cm^{2}sec). The stratified ambient mass, driven by buoyant bubbles, is entrained into the plume mostly within a vertical cylinder with a diameter not larger than 8.0 cm and appears as a discrete property in space. In contrast to the entraining mass flux, the peeling mass flows mostly out of the plume asymmetrically at the middle and upper parts of the plume. This asymmetry may result from a stratified ambient instability and the effects of the rectangular tank boundaries. For both peeling flux and entraining flux, we further found, as shown in Fig. 3, that they consist of an inner part in which fluid moves upward ($w > 0$, Fig. 3(a-1) and 3(b-1)), and an outer part in which fluid moves downward ($w < 0$,

Fig.3(a-2) and 3(b-2)). In the inner part, the mass flux field, including both the entraining-in and peeling-out regions, presents as a core of the plume in three-dimensional space very close to the center line of the computation domain, along the edge of the air bubble plume. Annularly, the inner-peeling-out mass flux (Fig. 3a-1, w>0) has approximately the same spatial scale as that of the re-entraining-in mass flux (Fig.3b-2, w<0). This counter mass flux-pair results from the direct interaction between drag force due to rising air bubbles and buoyant resistance ($\partial\rho/\partial z > 0$) due to the hydrostatic stability of the stratified ambient fluid. This creates some eddies that tumble vertically. Another part of the peeling-out mass flux, seen as the outer peeling-out mass flux with a relatively slow downward velocity, however, penetrated horizontally to form the multi-layer outlines of the plume in a relatively large annular scale. These will finally impinge on the tank wall and induce large-scale motion.

The mean mass flux averaged horizontally for each section, namely the inner and outer parts of entraining-in and peeling-out, is shown in Fig. 4 for qualitative comparison of the order of magnitude. From this figure, we can clearly identify that the inner-peeling-out mass flux and re-entraining-in mass flux are approximately of the same order at each horizontal sections, while the outer peeling-out mass flux and inner entraining-in mass flux are on the same order as well. This implies that in the stratified ambient plume there exist two regions of momentum balance, one consisting of small-scale turbulent eddies, as mentioned above, located vertically at the edge of the air bubble plume, and the other consists mainly of momentum produced from drag force in the inner plume as bubbles moving into outer part of plume to support the large scale motion of the stratification fluid. As shown in Fig. 5, less than 15 percent of the entraining-in and peeling-out mass flux was involved the inner turbulent tumbling processes (peeling-mass-out and re-entraining-in), while over 85 percent of the entraining-in mass flux was involved in large-scale motion. This result might provide useful for constructing and modifying theoretical plume models (McDougall, 1978; Asaeda and Imberger, 1993).

For time evolution processes, we sampled the simulation results at 312.0 seconds and 512.0 seconds. For the dispersion phase, namely the air bubbles, the plumes at these two times with the density fields as the background on the vertical central section ($y = 0.5$ m) are visualized numerically in Fig. 6 in terms of the air bubble void fraction. There is virtually no change from the early stage to the later stage, indicating that the air bubble plume reaches a relatively steady state earlier than does the stratified fluid plume. Under the present simulation conditions, the air bubble plume seems to depend less on variations in the outer stratification fluid flow field and instead is governed locally by the inner (core) dynamics that result from the direct interaction between the two phases.

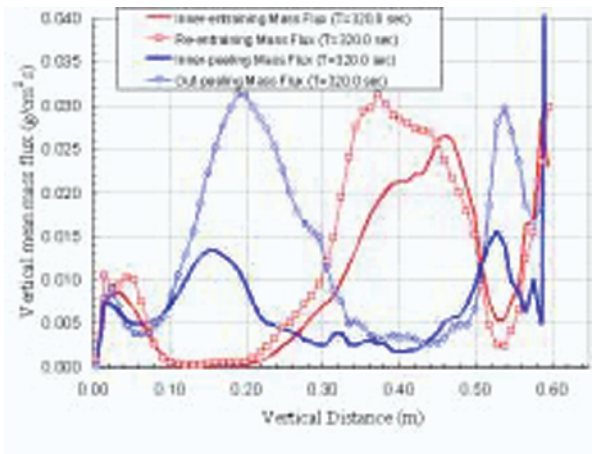

Fig. 4. Vertical profiles of inner- and out entraining-in mass flux and inner- and out peeling-out mass flux at 312.0 seconds.

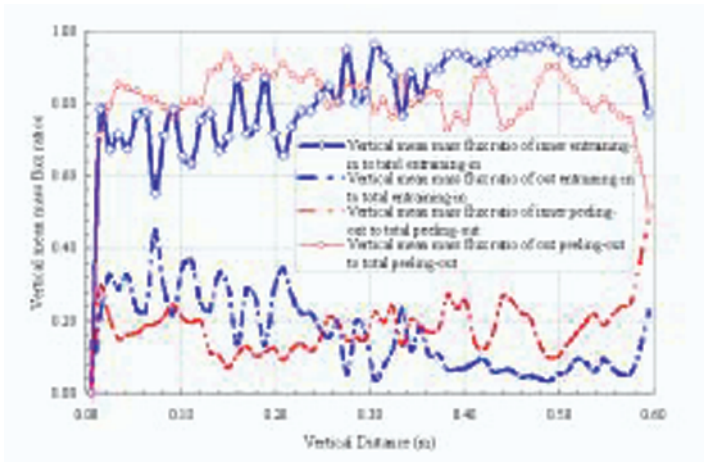

Fig. 5. Percentages of inner- and out entraining-in and peeling-out mass flux to total mass flux, respectively.

In contrast to the air bubble plume, the density field of the stratified fluid evolved gradually toward a more destratified field. Due to the continual injection of air bubbles, ambient fluids of greater density were lifted up from the lower part of the tank and the lighter fluid at the top of the tank was drawn down by free surface entraining flows to form a new dynamic density field. When we look at the streamlines for these two density fields, the stratified ambient fluid moved symmetrically inside the tank at the early stage (T=312.0 seconds, Fig. 6(c)) in which four large-scale vortexes appeared at each side of the plume centerline.

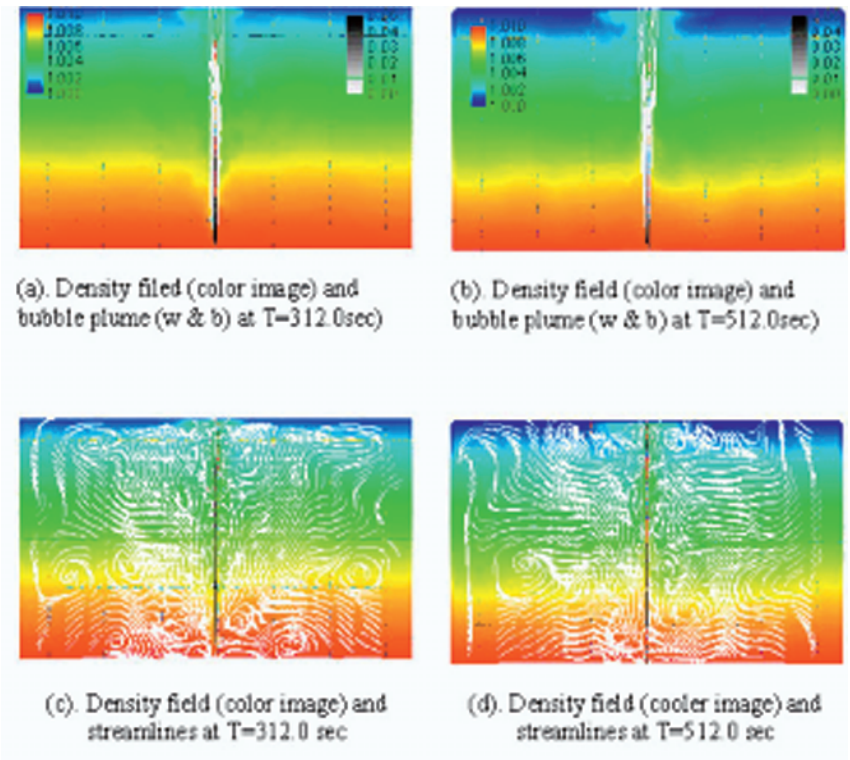

Fig. 6. Density fields, air bubble plumes (air bubble void fraction), and streamlines of stratified ambient at 312.0 seconds and 512.0 seconds after start of air bubble injection.

In the later stage (T=512.0 seconds, Fig. 6 (d)), this symmetrical flow field seems to be disturbed by flows in the outer parts, and is dominated mainly by the flows affected by the solid rectangular walls to which fluids penetrated horizontally due to local density differences being diminished, as mentioned above.

To further illustrate the stratification characteristics of the ambient fluid, the isosurfaces of the density fields at three vertical layers are given in Fig. 7 associated with the density field on central-vertical section at time of 892.0 seconds. These density fields are representative of the inner and outer structure of the plume, as indicated by the mass flux. Around the central region, which we refer to as the inner part of the plume, the isodensity surface was wrinkled by small turbulent eddies, which result from the interaction between inner peeling-out mass flux and re-entraining-in mass flux, even though the original sources are from the two phase interactions, the slip velocity between air bubble and stratified fluid, and the static/dynamic stability of the fluid stratification. On the outside portion of the isodensity surfaces, the wrinkles appeared to be large-scale and wave-like in shape. These further illustrate large-scale movement of the stratified fluid on the annular-out regime of the plume.

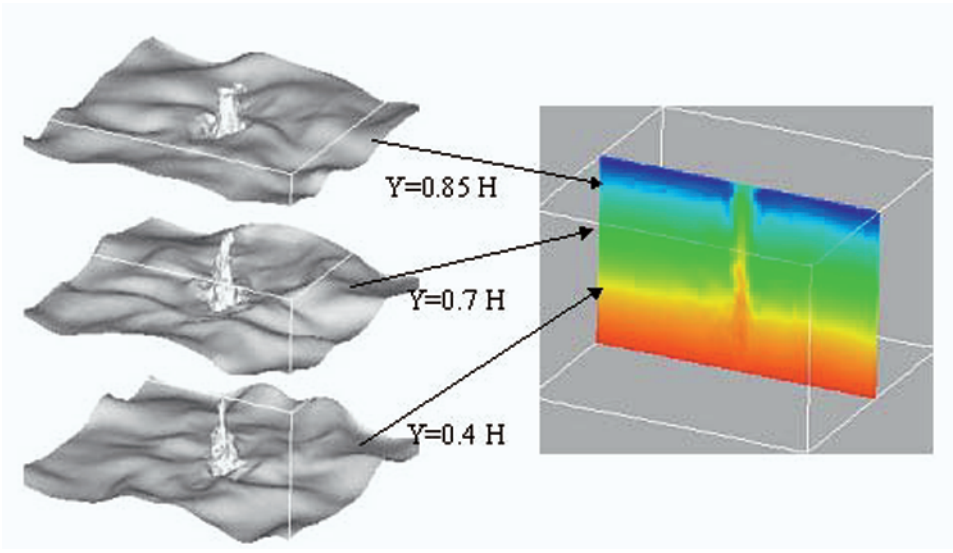

Fig. 7. Isodensity surfaces at three horizontal sections.

5. Conclusion

Two-phase flow theory and large-eddy simulation technologies were applied to the numerical visualization of two-phase plume formation and evolution in a stratified ambient. The model was validated using experimental data obtained for mean vertical density profiles. Both the numerical prediction and experimental data are in good agreement from the early to later stages of plume evolution. For the stratified ambient plume, numerical visualization results indicate not only a multi-layer outline, which corresponds to the overall geometry of the plume as determined empirically (Asaeda and Imberger, 1993), but also the inner structure and formation mechanism as well. The formation mechanism of tumbling turbulent eddies arises from the interaction between an inner peeling-out mass flux and an outer entraining-in mass flux, which have the same order of magnitude and appear in the same region at the edge of the air bubble plume. The mass flux involved

in these tumbling turbulent eddies, for both entraining-in and peeling-out, is less than 15 percent of the total mass flux. The plume characteristics are easily observable when visualized in terms of the isosurfaces of the density fields.

Simulations using the model developed in this study also show the potential for further engineering applications, for example, simulation of CO_2 sequestration in the oceans.

Acknowledgements

This study is a part of the investigation of the CO_2 Ocean Sequestration Project managed by the Research Institute of Innovative Technology for the Earth (RITE) and funded by the New Energy and Industrial Technology Development Organization (NEDO), Japan.

References

Asaeda, T. and Imberger, J., Structure of Bubble Plumes in Linearly Stratified Environments, J. Fluid. Mech. 249, (1993), 35-57.

Haungan, P. M., Thorkildsen, F. and Alendal, G., Dissolution of CO_2 in the Ocean, Energy Convers. Mgmt. 36, (1995), 461-466.

Johansen. ∅., Deep Blow – a Lagrangian Plume Model for Deep Water Blowouts, Proceeding of 3rd International Marine Environmental Modeling Seminar, Lillebammer. (1999), 97-103.

Lesieur, M. and Métais, O., New Trends in Large-eddy Simulations of Turbulence, Annu. Rev. Fluid. Mech. 28, (1996), 45-87.

Liro, C. R., Adams, E. E. and Herzog, H. J., Modeling the Release of CO_2 in the Deep Ocean, Energy Conserv. Mgmt. 33(5-8), (1992), 667-674.

Lam, K. and Banerjee, S., On the Condition of Streak Formation in a Bounded Turbulent Flow, Physics of Fluids A 4, (1992), 306-320.

McDougall, T. J., Bubble Plumes in Stratified Environments, J. Fluid Mech. 85, (1978), 655-672.

Schlodow, S. D., Bubble Plume Dynamics in a Stratified Medium and the Implications for Water Quality Amelioration in Lakes, Wat. Resour. Res. 28, (1992), 313-321.

Sirignano, W. A., The Formulation of Spray Combustion Models' Resolution Compared to Droplet Spacing, ASME, J. of Heat Transfer, 108, (1986), 633-639.

Socolofsky, S. A, Laboratory Experiments of Multi-phase Plumes in Stratification and Cross Flow, Ph.D Thesis, Dept. of Civil and Environmental Eng, MIT, Cambridge, MA. U.S.A., (2000).

UNESCO, Tenth Report of the Joint Panel on Oceanographic Tables and Standards, UNESCO Technical Papers in Marine Science, 36, (1981), 24-29.

Van Doormaal, J. P. and Raithby, G. D., Enhancement of the SIMPLE Method for Predicting Incompressible Fluid Flows, Numer. Heat Transfer, 7, (1984), 147-163.

Author Profile

Baixin Chen: He received his Ph.D. degree in Mechanical Engineering in 1989 from Dalian University of Technology, then worked as an academic staff in the University till 1998 when he turned to work for Research Institute of Innovative Technology for the Earth (RITE), Japan. His research interests include the numerical simulation of turbulent multi-phase fl9ows in I.C. engines and Large-eddy simulation of environmental flow. He also interested in the optical diagnostics on physic-chemical properties of fluids and measurement technologies of CO_2 hydrate clathrate formation and dissolution.

Yongchen Song: He received his MSc (Eng) and Ph.D. in Mechanical Engineering in1989 and 1992 respectively from Dalian University of Technology. He then was pointed as an academic staff of the University till the year of 1996 when he began to work in Nagoya University and National Environmental Institute Japan as a researcher. Since year 2000, he had been worked for Research Institute of Innovative Technology for the Earth (RITE), Japan as a senior researcher. His research interests are the investigations of optical-based diagnostics on fluid follows and on physic-chemical properties and of CO_2 sequestration technology.

Masahiro Nishio: He received his MSc (Eng) in Chemical Engineering in1987 from Yokohama National University. He also received Ph.D. in Chemical Engineering in 1990 from Yokohama National University, then worked as a researcher for Mechanical Engineering Laboratory, AIST, MITI. He has been working in the National Institute of Advanced Industrial Science and Technology (AIST) Tsukuba as a senior research scientist. His research interests are CO_2 sequestration technology, Crystal Growth of Gas Hydrate and Flow Visualization.

Satoshi Someya : He received his Ph.D. degree in Nuclear Engineering in 1998 from University of Tokyo, then worked as a Research Fellow of New Energy and Industrial Technology Development Organization (NEDO) (1998-2000) in the Mechanical Engineering Laboratory of AIST. He has worked in National Institute of Advanced Industrial Science and Technology (AIST) Tsukuba as a temporary researcher. He is a member of Thermal Engineering Research Group. His research interests are Crystal Growth, CO_2 sequestration, Flow Induced Vibration and Flow Visualization.